

Quantum effects in the dissociative adsorption of hydrogen

Axel Groß

Physik-Department T30, Technische Universität München, D-85747 Garching, Germany

(Received 3 December 1998; accepted 3 February 1999)

Three-dimensional quantum and classical dynamical calculations of the dissociative adsorption of hydrogen have been performed, in which, besides one reaction path coordinate, the lateral degrees of freedom of the hydrogen center of mass were taken into account. These calculations were compared to results obtained by classical and quantum sudden approximations, which assessed the importance of tunneling, zero-point effects, and also steering in the dissociative adsorption of hydrogen. For energies below the minimum barrier height, tunneling is of course the relevant mechanism for dissociation, but above the minimum barrier height quantization and zero-point effects become more prominent. Zero-point effects suppress the dissociation probability; however, for energies slightly above the minimum barrier height, steering of the particles is only operative in the quantum dynamics and can thereby almost compensate the suppression of the quantum sticking probabilities due to zero-point effects, compared to the classical calculations. The consequences of these findings with respect to the concept of zero-point corrections in order to obtain effective quantum barrier heights are discussed. The results presented in this study should be relevant for the reaction and propagation dynamics in all systems containing hydrogen. © 1999 American Institute of Physics. [S0021-9606(99)70117-0]

I. INTRODUCTION

The dynamics of hydrogen moving on multidimensional potential energy surfaces (PES) plays an important role in many research fields: in organic chemistry, in growth processes and the passivation of semiconductor devices, in the hydrogen gas storage in metals, in reactions involving water, in biological systems, just to name a few. Although recently it has become possible to perform six-dimensional quantum studies of reactions involving hydrogen,¹⁻⁵ these quantum dynamical methods are far away from being able to handle systems involving tens or hundreds of atoms in the foreseeable future. In order to perform dynamical studies on those systems, one still has to use classical molecular dynamics methods.

The shortcomings in using classical mechanics to simulate dynamical processes have of course been known for a very long time, namely the problem of tunneling and zero-point effects, and there have been attempts to incorporate these effects into classical mechanics (see, e.g., Refs. 6,7). But these attempts have, at least to my knowledge, not found wide recognition. Due to the development of efficient first-principles total-energy methods the determination of reliable potential energy surfaces and high-dimensional *ab initio* molecular dynamics simulations have become possible.⁸ There will be a growing number of *ab initio* molecular dynamics studies where systems involving hydrogen will be treated. In these molecular dynamics studies the dynamics of hydrogen is treated classically. Hence there is a need for assessing the importance of quantum effects in dynamical processes. Besides, the study of quantum effects is of course of fundamental interest. Only the recent progress in performing high-dimensional quantum studies has made it possible to address

the difference between quantum and classical calculations in realistic systems.⁹⁻¹³

Of particular importance are those quantum effects on reaction probabilities that cannot be explained by classical mechanics because they detect quantum effects experimentally. Six-dimensional dynamical quantum studies of the dissociation of H₂ under normal incidence on the reactive surface Pd(100), for example, yielded large oscillations in the sticking probability as a function of the kinetic energy.² These oscillations have been shown to be due to threshold effects, namely the opening up of new diffraction and rotational excitation channels in the scattering of hydrogen on the periodic surface.^{14,15} Although these oscillations have been searched for,^{16,17} they have not yet been found since the coherence of the scattering event is very sensitive to the initial conditions. They can very easily be suppressed by surface imperfections which on a reactive surface are caused, e.g., by the adatoms created during the course of the experiment; in addition, in non-normal incidence as used in the experiment^{16,17} the quantum oscillations are much smaller caused by the reduced symmetry of the scattering event.^{10,15}

In this study focus is not on quantum effects due to the periodicity of the surface, but on more local effects occurring within the surface unit cell. This particular investigation was motivated by the results of a recent six-dimensional quantum and classical *ab initio* molecular dynamics study of the dissociative adsorption of hydrogen at the (2×2) sulfur-covered Pd(100) surface³ in which the differences between quantum and classical results for the sticking probability were astonishingly small for kinetic energies close to the minimum barrier height. The complexity of the six-dimensional dynamics makes it rather difficult to disentangle the different contributions like tunneling, zero-point effects, or diffraction that lead to the differences between classical and quantum dy-

namics. Therefore, three-dimensional classical and quantum dynamical calculations have been performed on a model potential which has, however, features that are rather similar to the $\text{H}_2/\text{S}(2\times 2)/\text{Pd}(100)$ PES. Performing restricted dynamical calculations and changing the parameters of the model potential make it possible to analyze the classical and quantum dynamics in a well-defined manner. Quantum and classical dynamical calculations have been carefully compared with results obtained by quantum and classical sudden approximations which assess the importance of tunneling, zero-point effects, and also steering in the dissociative adsorption of hydrogen. It turns out that tunneling is of course important for energies below and close to the minimum barrier height, whereas quantization and zero-point effects are more prominent for energies above the minimum barrier height. However, steering of the particles in the quantum calculations, which is almost absent in the classical dynamics for energies close to the barrier height, compensates for the suppression of the quantum sticking probabilities due to zero-point effects, in particular if the zero-point energies associated with the single frustrated modes are below 25 meV. This means that the concept of zero-point corrections that are added to the barrier height in order to obtain an effective barrier height does not necessarily give the correct description of the quantum effects. Furthermore, isotope effects were examined in the quantum dynamics. The results presented in this study should be relevant for the reaction and propagation dynamics in all systems containing hydrogen.

II. COMPUTATIONAL DETAILS

In this three-dimensional study the following hydrogen degrees of freedom are considered: One reaction path coordinate s that, for $s \rightarrow \infty$ corresponds to the hydrogen center-of-mass distance from the surface and for $s \rightarrow -\infty$ to the interatomic distance between the two hydrogen atoms *on* the surface, i.e., a movement along the reaction path coordinate from ∞ to $-\infty$, describes a dissociative adsorption event. The other degrees of freedom taken into account are the two lateral degrees of freedom X and Y of the hydrogen center-of-mass. The vibrational and rotational modes of the molecule have been neglected. That means that in this study we focus on modes—the lateral modes of the hydrogen center of mass—that are associated with rather low quantization energies (see below). Traditionally in dissociation studies the hydrogen vibrational motion has been at the center of attention.^{18–20} However, since the vibrational motion is in general the fastest mode in the dissociation process, this mode follows the process almost adiabatically, both quantum mechanically²¹ as well as classically.⁹ Therefore the vibrational motion can be treated as an adiabatic invariant and its actual dynamics be neglected. Another motivation for concentrating on the hydrogen center-of-mass degrees of freedom is the fact that this study also becomes relevant for any molecular dynamics calculation involving *atomic* hydrogen.

The PES has been chosen to have similar features as the PES for the hydrogen dissociation on the (2×2) sulfur covered Pd(100) surface:²² The minimum barrier has a height of 0.09 eV, the adsorption energy is $E_{\text{ad}} = 1$ eV, the square surface unit cell has a lattice constant of $a = 5.5 \text{ \AA}$, and the

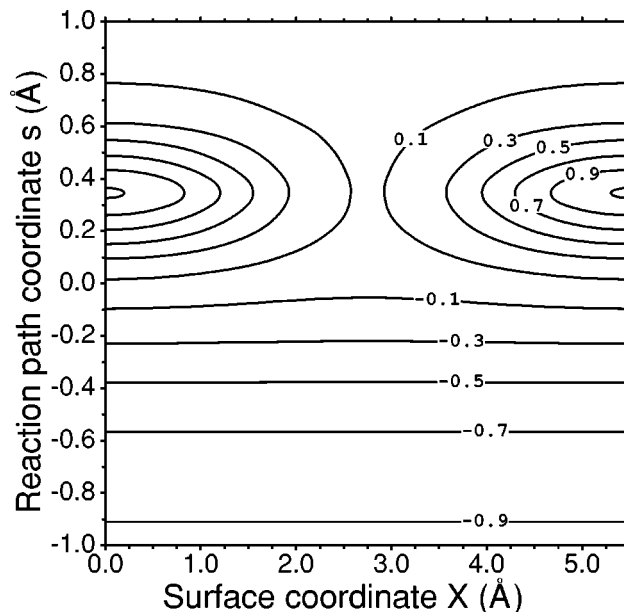


FIG. 1. Contour plot of the PES along a two-dimensional cut with the corrugation amplitude $E_G = 2$ eV (see text). The PES is shown as a function of the reaction path coordinate s and the surface coordinate X . The reaction path coordinate s corresponds for $s \rightarrow \infty$ to H_2 in the gas phase, and for $s \rightarrow -\infty$ to the two H atoms adsorbed dissociatively on the surface. The other surface coordinate Y is chosen to be $Y = 2.75 \text{ \AA}$ so that at $X = 2.75 \text{ \AA}$ the minimum barrier position is located. Energies are in eV per H_2 molecule. The contour spacing is 0.2 eV.

corrugation amplitude is similar. All the length scales are also derived from the $\text{H}_2/\text{S}(2\times 2)/\text{Pd}(100)$ PES. The 3D-PES is given by

$$V(s, X, Y) = V_0(s) + V_{\text{corr}}(s, X, Y). \quad (1)$$

$V_0(s)$ is the potential along the minimum energy path:

$$V_0(s) = E \cosh(\lambda s)^{-2} + F [\tanh(\lambda s) - 1]. \quad (2)$$

The parameter F is related to the adsorption energy via $F = \frac{1}{2}E_{\text{ad}}$, and E is chosen in such a way as to give a minimum barrier of height $E_b^{\text{min}} = 0.09$ eV. The length scale of the minimum energy path is determined by $\lambda = 0.45 \text{ \AA}^{-1}$. The position of the minimum barrier along the reaction path can be derived from Eq. (2) and is given by

$$s_{\text{barr}} = \frac{1}{\lambda} \operatorname{arctanh} \left(\frac{F}{2E} \right). \quad (3)$$

$V_{\text{corr}}(s, X, Y)$ determines the variation of the height of the barrier:

$$V_{\text{corr}}(s, X, Y) = E_G \cosh(\gamma(s - s_{\text{barr}}))^{-2} \times \frac{1}{4} [2 + \cos(G_X X) + \cos(G_Y Y)], \quad (4)$$

where

$$G_X = G_Y = \frac{2\pi}{a}, \quad (5)$$

are the basis vectors of the two-dimensional reciprocal lattice. The length parameter $\gamma = 1.25 \text{ \AA}^{-1}$ controls the thickness of the additional barriers due to the corrugation. Figure 1 shows a contour plot of the PES along the reaction path

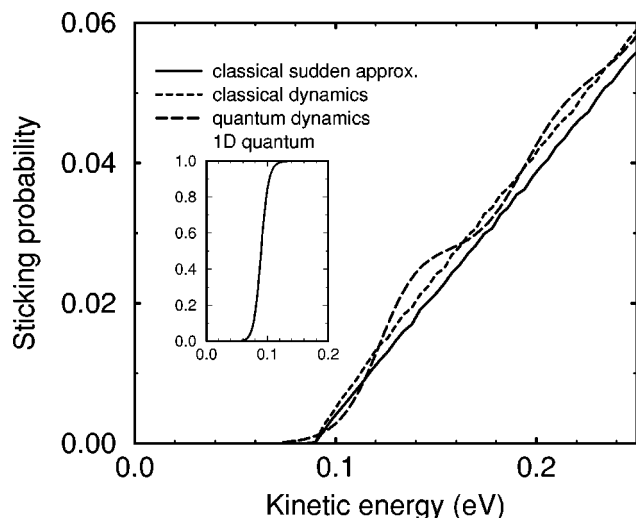


FIG. 2. Sticking probability versus kinetic energy for a H_2 beam under normal incidence obtained by three-dimensional calculations with $E_G = 2$ eV (see text). Full line: barrier distribution, which corresponds to the sticking probability in the classical sudden approximation; dashed line: classical sticking probability; long-dashed line: quantum sticking probability. The inset shows the 1D quantum sticking probability which corresponds to the sticking probability at a noncorrugated surface with just the minimum barrier.

coordinate s and the surface coordinate X . This two-dimensional cut through the three-dimensional PES includes the minimum barrier position. As Fig. 1 illustrates, the PES is parametrized in such a way that only the barrier height varies within the surface unit cell, but not the barrier position, i.e., only the so-called energetic corrugation is considered.^{23,24} The size of this variation is given by E_G .

The quantum dynamical calculations are performed by solving the time-independent Schrödinger equation in a coupled-channel scheme using the concept of the *local reflection matrix* (LORE).^{25,26} The classical trajectory calculations are carried out on *exactly* the same PES as the quantum dynamical calculations. The equations of motions are numerically integrated with the Bulirsch–Stoer method with a variable time-step.²⁷ The energy conservation per molecular dynamics run was fulfilled to 0.1 meV. The sticking probability is determined by averaging over a sufficient number of trajectories, which is typically 5000 in this study.

III. RESULTS AND DISCUSSION

The sticking probability of a hydrogen beam under normal incidence has been determined in two sets of calculations with different values of the energetic corrugation amplitude E_G . The particular values have been chosen in order to make the corrugation comparable to the $H_2/S(2 \times 2)/Pd(100)$ system. The first set of calculations have been done with $E_G = 2$ eV and is shown in Fig. 2. In addition, the quantum mechanical sticking probability for the noncorrugated surface with just the minimum barrier is shown in the inset and is denoted by 1D quantum results. The 1D sticking curve rises much more rapidly than the 3D curves. Indeed, at $E = 0.09$ eV this curve has its point of inflection at a sticking probability of 0.5. Figure 2 confirms the fact that at a corru-

gated surface it is the barrier distribution and not the barrier width that determines the slope of the sticking curve.²⁸

The integrated barrier distribution $P_b(E)$ is shown by the full line in Fig. 2. It is the fraction of the configuration space for which the barrier towards dissociative adsorption is less than E ; it corresponds to the sticking probability in the classical sudden approximation because it determines the fraction of classical particles that can cross the barrier region if these particles are not diverted by the PES. This approximation is also the basis of the so-called ‘hole model’²⁹. In Fig. 2 the integrated barrier distribution is denoted by ‘classical sudden approximation;’ it is given by

$$P_b(E) = \frac{1}{A} \int \Theta(E - E_b(X, Y)) dX dY, \quad (6)$$

where $E_b(X, Y)$ is the barrier height for fixed X and Y coordinates. A is the area of the surface unit cell and Θ the Heaviside step function. The classical sticking probabilities are larger than the results according to the classical sudden approximation. This is due to steering of particles to lower barrier sites caused by the corrugation of the potential.^{2,30} The quantum sticking probability shows a steplike structure. This is a well-known quantum effect caused by quantized states at the transition state.^{12,31} This phenomenon is closely related to the zero-point energies. At the minimum barrier position the wave function has to pass through a narrow valley of the corrugated PES. This leads to a localization of the wave function and thereby to a quantization of the allowed states that can pass through this valley. In the harmonic approximation the energy levels correspond to harmonic oscillator eigenstates which are equidistant in energy. Their spacing, $\hbar \omega$, is determined by the curvature of the PES in the coordinates perpendicular to the reaction path. For our model potential these energies can be determined analytically; at the minimum barrier position they are

$$\hbar \omega_G = \hbar G \sqrt{\frac{E_G}{2m}}. \quad (7)$$

For H_2 and $E_G = 2$ eV we obtain an energy of $\hbar \omega_G = 37$ meV for any of the two modes in X and Y direction. For normal incidence the incident wave function is even with respect to the minimum barrier position. The symmetry of the surface unit cell then only allows transitions between quantized states with the same symmetry, i.e., only transitions with $\Delta E = 2\hbar \omega_G = 74$ meV. Indeed the steplike structure of the quantum sticking probability in Fig. 2 has a step width of approximately 75 meV confirming the influence of these quantized states at the barrier position.

From a theoretical point of view it is very interesting and instructive to study the limiting case of an infinitely thick barrier. Therefore the three-dimensional quantum dissociation probability has also been determined for a PES given by

$$V(s, X, Y) = \begin{cases} V_0(s) + V_{\text{corr}}(s, X, Y) & s \geq s_{\text{barr}} \\ V_0(s_{\text{barr}}) + V_{\text{corr}}(s_{\text{barr}}, X, Y) & s < s_{\text{barr}} \end{cases}, \quad (8)$$

i.e., for $s \geq s_{\text{barr}}$ the potential corresponds to the situation shown in Fig. 1, but for $s < s_{\text{barr}}$ the potential along the reaction path coordinate and also the corrugation are constant.

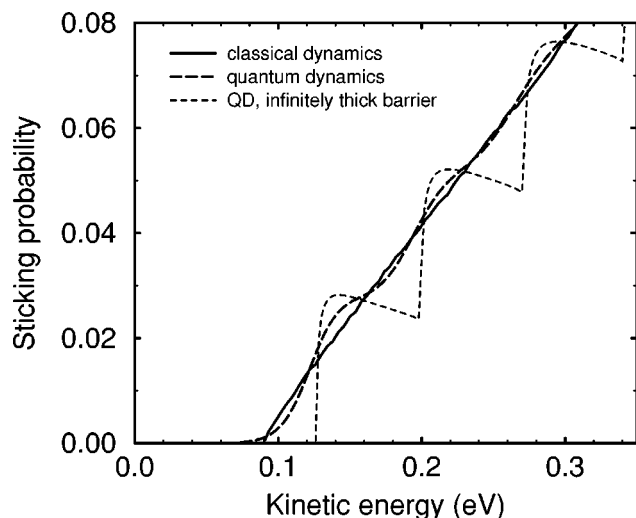


FIG. 3. Sticking probability versus kinetic energy for a H_2 beam under normal incidence obtained by three-dimensional quantum dynamical (QD) calculations with $E_G=2$ eV for an infinitely thick barrier according to Eq. (8) (thin dashed line) compared to the classical (solid line) and the quantum dynamical calculation (long-dashed line) for the barrier situation of Fig. 1.

The quantum results for this infinitely thick barrier are compared to the classical and quantum results for the regular barrier in Fig. 3. At the infinitely thick barrier the quantum dissociation probability now exhibits almost a “real” staircase structure. The infinitely thick barrier acts as a wave guide where only quantized portions of particles can be transmitted. The separation of the steps can be accurately determined; it turns out that the separation is ≈ 72 meV, which is a little bit less than $2\hbar\omega_G=74$ meV, and becomes smaller with increasing energy. This is a consequence of the anharmonicity of the cosine corrugation potential. The fact that the sticking probability slightly decreases on the plateaus can be explained by the steering effect: with increasing energy less intensity of the incoming particles can be focused into the quantized states.

Another effect of the quantization of the levels becomes very clear. The frustrated translational modes parallel to the surfaces are also associated with zero-point vibrations. In order to propagate, the kinetic energy of the incident wave function has to be larger than the minimum barrier height plus the sum of zero-point energies in the modes perpendicular to the reaction path. For the potential with $E_G=2$ eV each frustrated translational motion results in a zero-point energy at the minimum barrier position of $\frac{1}{2}\hbar\omega_G=18.5$ meV which means that the effective minimum barrier is increased by $2 \times \frac{1}{2}\hbar\omega_G=37$ meV. This additional barrier height is said to be due to the so-called zero-point corrections (ZPC). These ZPC result in an effective minimum barrier height of 0.127 eV, and indeed, at exactly this energy the dissociation probability at the infinitely thick barrier rises abruptly.

One further interesting phenomenon is the fact that at the thresholds the sticking probability at the infinitely thick barrier becomes even larger than the sticking probability at the thin barrier. Naively, one would expect that due to additional tunneling the sticking probability at the thin barrier is for all energies larger than at the infinitely thick barrier. The reason

for this lies in the quantum reflection for energies larger than the barrier height. At thin barriers this quantum reflection is stronger than at thick barriers. Apparently the hindering influence of the quantum reflection is stronger than the promoting effect of additional tunneling for the propagation on the corrugated PES. Hence for the comparison of two quantum results the consideration of quantum reflection is important. However, the overall promoting effect of tunneling at the corrugated PES at these particular energies with respect to the classical results is still stronger than the hindering effect of the quantum reflection. This becomes evident from the fact that the classical sticking probability is smaller than the quantum ones for energies at which new quantized states at the transition state become accessible.

The question arises whether some kind of a steplike structure in the dissociation probability might be observable in the experiment. The calculations presented here are performed in a restricted geometry. In six dimensions the frustrated hydrogen rotations at the transition state also lead to a quantized structure.¹² Together with the frustrated parallel translation this causes a manifold of possible quantized levels which might smear out the steplike structure. However, the 6D quantum sticking probability of $H_2/S(2 \times 2)/Pd(100)$ also exhibits some steplike structure which is absent in the classical calculations.³ In contrast, in the 6D quantum calculations for $H_2/Cu(100)$ such a structure is hardly resolvable.⁴ Certainly an experimental verification of the existence of the quantized states requires a rather monoenergetic beam and a well-defined, perfectly ordered surface which should be fairly cold in order to suppress the influence of thermal fluctuations. This certainly represents an experimental challenge.

Coming back to the zero-point corrections, it is a common concept that the effective minimum barriers for quantum particles should be modified by the zero-point corrections in order to incorporate quantum effects. However, a closer look at Fig. 2 reveals that for energies slightly larger than the minimum barrier height, indeed the quantum sticking probability at the regular thin barrier is suppressed with respect to the classical sticking probability, but the shift on the energy axis is much less than the ZPC of 37 meV. Interestingly enough, the kinetic energy associated with the first point of inflection of the quantum sticking curve in Fig. 2 is rather close to the minimum barrier height plus the ZPC. Close to this point the quantum and the classical sticking curves cross; the quantum sticking probability becomes larger than the classical one.

In order to clarify the nature of the dissociation dynamics in this energy regime, in Fig. 4 the region around the minimum barrier height has been enlarged. In addition to the classical and quantum sticking probabilities and the classical sudden approximation, results have also been plotted according to a quantum sudden approximation or quantum hole model (see, e.g., Ref. 32). In this approximation the sticking probability is given by

$$S_{\text{sud}}^{\text{qm}}(E_{\text{kin}}) = \int S^{1D}(E_{\text{kin}}, E_b) p_b(E_b) dE_b, \quad (9)$$

i.e., $S_{\text{sud}}^{\text{qm}}$ corresponds to an integral over 1D sticking probabilities with different barrier heights E_b , weighted by

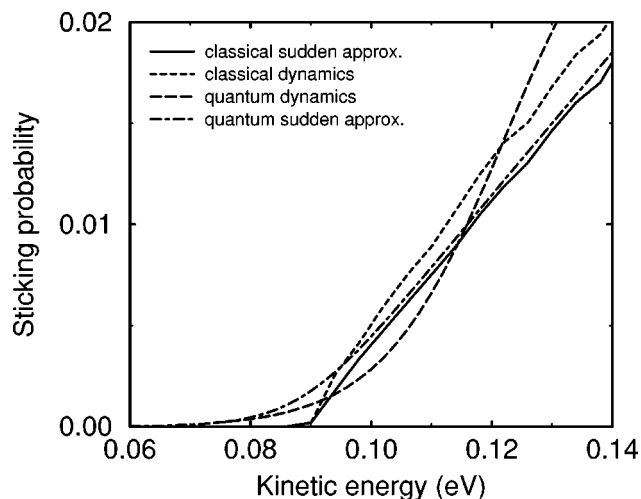


FIG. 4. Sticking probability versus kinetic energy for a H_2 beam under normal incidence obtained by three-dimensional calculations with $E_G = 2$ eV (see text). The notation corresponds to Fig. 2 except for the fact that the dot-dashed line shows the results of the quantum sudden approximation.

$p_b(E_b)$. Here $p_b(E)$ corresponds to the probability of finding a barrier with a height between E and $E + dE$, i.e., it can be derived from the integrated barrier distribution $P_b(E)$ via

$$p_b(E) = \frac{dP_b(E)}{dE}. \quad (10)$$

In practice, the integral over the barrier distribution in Eq. (9) has been replaced by a sum for which 75 sticking curves for 1D barriers with heights ranging from 90 to 390 meV have been determined. This quantum sudden approximation corresponds to the quantum sticking probability at the corrugated surface without any ZPC and steering effects.

Due to the ZPC one expects the effective barrier in the quantum calculations to be higher by 37 meV compared to the classical calculations. This causes a suppression of the sticking probability. One compensating mechanism is tunneling because it enhances the quantum transmission probability with respect to the classical one. However, the comparison between quantum and sudden approximation in Fig. 4 yields that tunneling alone cannot account for a promoting effect that cancels the hindering effect of the ZPC. For energies above the minimum barrier height the sticking curve in the quantum sudden approximation is shifted by less than 5 meV to smaller energies compared to the classical sudden approximation.

Furthermore, if one compares the quantum sudden approximation and the actual 3D quantum dynamics, one notices that for kinetic energies below approximately 0.11 eV the actual 3D quantum dynamical sticking probability is below the quantum sudden approximation. This indicates the influence of the zero-point effects. However, again the two sticking curves are not shifted on the energy axis by a value corresponding to the ZPC of 37 meV, but by only approximately 10 meV, although in both methods tunneling is taken into account. Thus there has to be another promoting mechanism except for tunneling *alone* that can compensate for the

suppression of the quantum sticking probability due to zero-point effects for energies close to the minimum barrier height.

There is only one promoting mechanism left that can counterbalance the zero-point effects, namely, dynamical steering.^{2,30} particles with unfavorable impact points are steered to lower barrier sites by the corrugated potential thus increasing the sticking probability. The promoting effect of steering leads to a shift of the quantum sticking curve that is smaller by 25 meV than expected. But steering is a general dynamical concept that is not restricted to quantum or classical dynamics. So why has steering not a similar promoting effect in the classical dynamics for energies slightly above the minimum barrier height, and why are the classical and quantum sticking probabilities rather close at these energies in spite of the zero-point effects?

The answer lies in the fact that in the classical dynamics, steering actually cannot be operative for energies slightly above the minimum barrier height. The reason is the following. Steering means that the particles are moved in a direction perpendicular to the reaction path. This also means that the particles acquire some kinetic energy perpendicular to the minimum energy path and this energy is then missing for the propagation across the minimum barrier position. This fact is evident in Figs. 2 and 4. For kinetic energies slightly above the minimum barrier height the sticking probabilities according to the classical sudden approximation and the classical dynamics calculations are almost the same. Steering becomes effective classically only at higher kinetic energies. In quantum dynamics in the tunneling regime, on the other hand, the traversing particles follow effectively the lowest energy propagation path because all other pathways are exponentially suppressed, as was shown in Ref. 24. This mechanism leads to efficient steering. Thus in contrast to the classical dynamics, in the quantum dynamics steering is also operative for energies below and at the minimum barrier height, i.e., also in the tunneling regime.

In conclusion, for energies close to the minimum barrier height the suppression of the quantum sticking probability due to zero-point effects compared to the classical sticking probability is counterbalanced by two promoting effects, namely tunneling *plus steering*. The consequences of all these quantum effects can almost cancel resulting in rather similar quantum and classical sticking probabilities for energies slightly above the minimum barrier height, as was for example found in the six-dimensional calculations of the sticking probability of H_2 at the (2×2) sulfur-covered Pd(100) surface.³

In order to check these findings discussed above, the calculations have been repeated for a different corrugation amplitude, namely for $E_G = 4$ eV. The results are plotted in Fig. 5 where the notation corresponds to Fig. 4. Now the quantum sticking probability shows a rather pronounced steplike structure. For $E_G = 4$ eV the frequency related to the two frustrated translation modes is $\hbar\omega_G = 52$ meV, so that the quantized states at the transition state should be separated by 104 meV. And indeed, the first two equivalent points of inflection of the quantum sticking curve in Fig. 5 are separated by a little bit more than 0.1 eV.

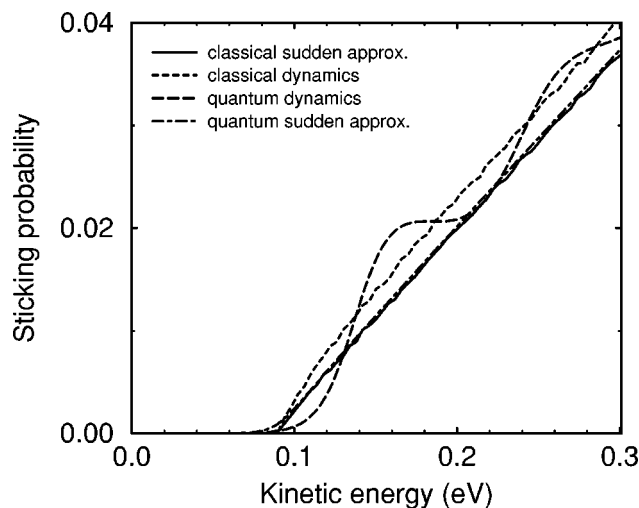


FIG. 5. Sticking probability versus kinetic energy for a H_2 beam under normal incidence obtained by three-dimensional calculations with $E_G=4$ eV (see text). The notation corresponds to Fig. 4.

The onset of the quantum sticking probability with respect to the classical sticking probability is now in fact clearly shifted to higher energies. At this surface with the larger zero-point energies of $\frac{1}{2}\hbar\omega_G=26$ meV in the single frustrated modes the hindering effect of the ZPC becomes obvious. Still, the shift is only approximately 20 meV which is much less than the ZPC of 52 meV for this PES with $E_G=4$ eV. And again, the first point of inflection of the sticking curve approximately coincides with the effective minimum barrier height of 0.142 eV including ZPC. Thus these results confirm the findings of the calculations with $E_G=2$ eV.

Finally also looked at is the isotope effect in the quantum sticking probability of a H_2 and a D_2 beam. Note that classically there can be no isotope effect because as a function of the kinetic energy different isotopes follow exactly the same trajectories in configuration space for the same PES.¹⁰ As a consequence, steering on a particular PES does not depend on the mass, just on the kinetic energy of the particles. In Fig. 6 the quantum sticking probabilities for a H_2 and D_2 beam moving on the PES with $E_G=4$ eV are shown. The classical sticking probability has been added as a guide to the eye. For D_2 the energetic separation between the quantized states at the transition state is smaller by a factor $1/\sqrt{2}$ compared to H_2 which is reflected in Fig. 6 by the smaller separation of the steps in the quantum sticking probability. Furthermore, for D_2 the suppression of the quantum sticking probability due to the zero-point effects should be less than for H_2 because the zero-point energies are smaller. On the other hand, for D_2 the promoting effect of tunneling should be smaller than for H_2 due to the higher mass. Since these two quantum effects have opposing consequences, the sign of the isotope effect is not obvious *a priori* and depends on the actual dynamics on a particular PES. The fact that for energies slightly above the minimum barrier height the quantum sticking probability of D_2 is larger than of H_2 shows that in this energy regime the zero-point effects are more prominent than the effects of tunneling. The stronger influence of

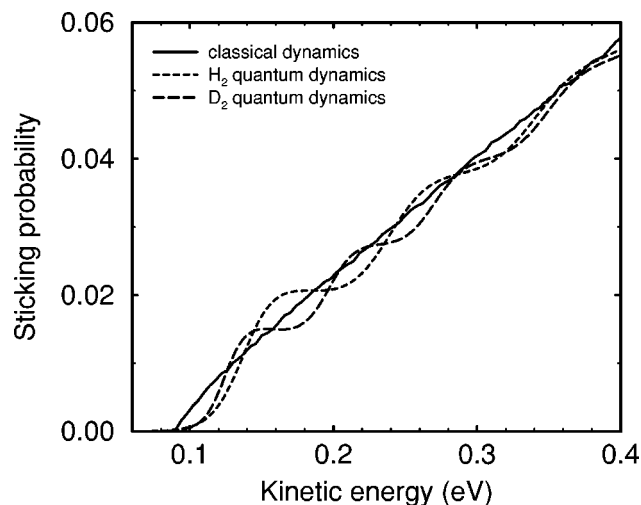


FIG. 6. Sticking probability versus kinetic energy for a hydrogen beam under normal incidence obtained by three-dimensional calculations with $E_G=4$ eV (see text). Full line: classical sticking probability which is independent of the mass as a function of the kinetic energy;¹⁰ dashed line: H_2 quantum sticking probability; long-dashed line: D_2 quantum sticking probability.

the zero-point effects is also reflected by the fact that for larger kinetic energies the quantum sticking probabilities fall below the classical sticking probabilities in spite of tunneling.

A technical note of caution should be added. In a coupled-channel scheme the wave-functions are expanded in a necessarily finite basis set. It is my experience that if this expansion is not converged as far as the basis set is concerned, then an additional artificial steplike structure in the quantum sticking probability results. Hence one has to be very cautious that a calculated steplike reaction probability is indeed caused by quantized states at the transition state and not an artifact of an insufficient expansion of the wave function.

IV. CONCLUSIONS

Three-dimensional quantum and classical dynamical calculations of the dissociative adsorption of hydrogen have been performed, in which besides one reaction path coordinate the lateral degrees of freedom of the hydrogen center of mass were taken into account. The results of these calculations were analyzed with the help of classical and quantum sudden approximations. The corrugation of the potential energy surface leads to the existence of quantized states at the minimum barrier position which are reflected by a steplike structure in the quantum sticking probabilities.

Due to zero-point effects the quantum sticking probability is suppressed compared to the classical sticking probability. However, in addition to tunneling for energies slightly above the minimum barrier height, steering of the particles to lower barrier sites leads to a promoting effect in the quantum dynamics, compared to the classical dynamics, because steering cannot be effective in this energy regime in the classical dynamics. Depending on the particular shape of the potential energy surface, these promoting effects can almost cancel the suppression of the sticking probability due to zero-point effects, in particular if the zero-point energies as-

sociated with the single frustrated modes are below 25 meV. This shows that the concept of adding zero-point corrections to the minimum barrier height in order to incorporate quantum effects has to be applied with caution and might overestimate the quantum effects.

ACKNOWLEDGMENTS

Useful discussions with Moritz Hilf, Eckhard Pehlke, and Matthias Scheffler are gratefully acknowledged. Special thanks go to Wilhelm Brenig for enlightening comments and a careful reading of the manuscript.

- ¹D. H. Zhang and J. Z. H. Zhang, *J. Chem. Phys.* **101**, 1146 (1994).
- ²A. Groß, S. Wilke, and M. Scheffler, *Phys. Rev. Lett.* **75**, 2718 (1995).
- ³A. Groß, C. M. Wei, and M. Scheffler, *Surf. Sci.* **416**, L1095 (1998).
- ⁴G. J. Kroes, E. J. Baerends, and R. C. Mowrey, *Phys. Rev. Lett.* **78**, 3583 (1997).
- ⁵J. Dai and J. C. Light, *J. Chem. Phys.* **107**, 1676 (1997).
- ⁶J. M. Bowman, B. Gazdy, and Q. Sun, *J. Chem. Phys.* **91**, 2959 (1989).
- ⁷W. H. Miller, W. L. Hase, and C. L. Darling, *J. Chem. Phys.* **91**, 2863 (1989).
- ⁸A. Groß, *Surf. Sci. Rep.* **32**, 291 (1998).
- ⁹A. Groß and M. Scheffler, *J. Vac. Sci. Technol. A* **15**, 1624 (1997).
- ¹⁰A. Groß and M. Scheffler, *Phys. Rev. B* **57**, 2493 (1998).
- ¹¹D. A. McCormack and G. J. Kroes, *Chem. Phys. Lett.* **296**, 515 (1998).
- ¹²A. D. Kinnersley, G. R. Darling, S. Holloway, and B. Hammer, *Surf. Sci.* **364**, 219 (1996).
- ¹³M. Kay, G. R. Darling, and S. Holloway, *J. Chem. Phys.* **108**, 4614 (1998).
- ¹⁴A. Groß and M. Scheffler, *Chem. Phys. Lett.* **263**, 567 (1996).
- ¹⁵A. Groß and M. Scheffler, *Phys. Rev. Lett.* **77**, 405 (1996).
- ¹⁶C. T. Rettner and D. J. Auerbach, *Phys. Rev. Lett.* **77**, 404 (1996).
- ¹⁷C. T. Rettner and D. J. Auerbach, *Chem. Phys. Lett.* **253**, 236 (1996).
- ¹⁸C. -M. Chiang and B. Jackson, *J. Chem. Phys.* **87**, 5497 (1987).
- ¹⁹D. Halstead and S. Holloway, *J. Chem. Phys.* **93**, 2859 (1990).
- ²⁰S. Küchenhoff, W. Brenig, and Y. Chiba, *Surf. Sci.* **245**, 389 (1991).
- ²¹A. Groß and M. Scheffler, *Chem. Phys. Lett.* **256**, 417 (1996).
- ²²C. M. Wei, A. Groß, and M. Scheffler, *Phys. Rev. B* **57**, 15572 (1998).
- ²³G. R. Darling and S. Holloway, *Surf. Sci.* **304**, 461 (1994).
- ²⁴A. Groß, *J. Chem. Phys.* **102**, 5045 (1995).
- ²⁵W. Brenig, T. Brunner, A. Groß, and R. Russ, *Z. Phys. B* **93**, 91 (1993).
- ²⁶W. Brenig and R. Russ, *Surf. Sci.* **315**, 195 (1994).
- ²⁷W. H. Press, B. P. Flannery, S. A. Teukolsky, and W. T. Vetterling, *Numerical Recipes* (Cambridge University, Cambridge, 1989).
- ²⁸A. Groß, B. Hammer, M. Scheffler, and W. Brenig, *Phys. Rev. Lett.* **73**, 3121 (1994).
- ²⁹M. Karikorpi, S. Holloway, N. Henriksen, and J. K. Nørskov, *Surf. Sci.* **179**, L41 (1987).
- ³⁰M. Kay, G. R. Darling, S. Holloway, J. A. White, and D. M. Bird, *Chem. Phys. Lett.* **245**, 311 (1995).
- ³¹D. C. Chatfield, R. S. Friedman, and D. G. Truhlar, *Faraday Discuss. Chem. Soc.* **91**, 289 (1991).
- ³²P. Kratzer, B. Hammer, and J. K. Nørskov, *Surf. Sci.* **359**, 45 (1996).